Theor Chem Acc (2010) 127:259–270
DOI 10.1007/s00214-010-0766-y

FEATURE ARTICLE

Hydrogen physisorption in metal–organic frameworks: concepts and quantum chemical calculations

German Sastre

Received: 26 March 2010 / Accepted: 6 May 2010 / Published online: 22 May 2010

Abstract Storage of hydrogen by physisorption in metal–organic frameworks is reviewed from the perspective of quantum chemistry. Concepts regarding the interaction of hydrogen with metals are revised and the specific features of metal–organic frameworks are explained. The influence of the type of inorganic cluster and hydrogen loading and its relation to hydrogen storage are analysed. Heats of hydrogen adsorption in previous studies are critically discussed and estimations are made regarding the adsorption strength needed for storage applications and how to approach commercial targets.

Keywords MOF · Hydrogen · Storage

1 Introduction

The design of new materials is strongly based on our knowledge of the general rules that dictate order at the short and long range in matter. The use of polytopic ligands and the synthesis of new metal clusters have allowed classical organometallic chemistry to expand from molecules to crystalline solids through the synthesis of metal–organic frameworks (MOFs). A proper choice of metallic clusters allows tridimensional structures to be formed where all the bonds are mainly covalent in character and this provides, together with the use of rigid organic molecules as ligands, the basis for the synthesis of rigid frameworks [1–4]. Framework robustness is a *sine qua non* condition for applications such as storage and catalysis and has led to name the subclass of MOFs within the wider class of coordination polymers. New synthesis procedures have allowed to obtain structures capable of maintaining structural integrity upon removal of the solvent used in the synthesis and upon repeated cycles of adsorption/desorption of guest molecules. MOFs, in general, do not allow molecular separation in terms of shape selectivity, as it is the case in zeolites, but selective adsorption is still possible through the chemistry of the adsorption, which can be tuned through the type of inorganic cluster forming part of the framework.

Storage applications require intermediate binding energies between two extreme cases: chemisorption and weak physisorption. Chemisorption of hydrogen—which occurs, for instance, in complex hydride systems, for example alanates—has the advantage that large hydrogen contents can be retained, but this leads to undesired slow desorption (due to slow kinetics) and excessive heat release. Weak physisorption, on the other hand, is observed in many metal–organic frameworks, where the main advantage of these materials is a high specific surface area but with the drawback of a low isosteric heat of adsorption, which means that maximum uptake can only occur at low temperatures (ca. 77 K). Efforts are currently ongoing in both directions: new complex hydrides with larger surface area and weaker adsorption sites, and metal–organic frameworks with larger (more negative) heats of adsorption. The latter is the subject of this review. Previous reviews [5–9] have considered different aspects of this topic, also including atomistic computational approaches [10]. In the present study we highlight some concepts as well as

Electronic supplementary material The online version of this article (doi:10.1007/s00214-010-0766-y) contains supplementary material, which is available to authorized users.

G. Sastre (✉)
Instituto de Tecnologia Quimica U.P.V.-C.S.I.C.,
Universidad Politecnica de Valencia, Av. Los Naranjos s/n,
46022 Valencia, Spain
e-mail: gsastre@itq.upv.es

quantum chemistry calculations focused on the physical chemistry of hydrogen adsorption at the inorganic cluster part of the MOF.

2 Hydrogen–hydrogen intermolecular interactions

Hydrogen–hydrogen intermolecular repulsions are particularly strong at short ranges, as known from its difficult compressibility, and storage applications require high hydrogen density. At the density of the liquid hydrogen, 70.99 g/L (at 20 K), a simple approximate calculation shows an average intermolecular H_2–H_2 separation of ca. 3.5 Å (see Electronic Supplementary Materials, ESM). At shorter distances, repulsion and electronic correlation become increasingly important. The overall interaction energy between two hydrogen molecules comes from three terms: short-range valence (overlap, exchange, Pauli) forces, long-range dispersion, and electrostatic quadrupole–quadrupole interactions. Quantum chemistry calculations regarding hydrogen storage materials (at a density approaching that of liquid hydrogen) need to take into account short-range repulsions, which means that electronic correlations effects play a significant role and an accurate evaluation of the short-range repulsive part of the H_2–H_2 interaction is needed. In post-Hartree–Fock methods, a correlation treatment through Møller-Pleset theory at the MP2 level is sufficient to describe H_2–H_2 interactions with the accuracy required in metal–organic systems. The calculated binding energy of the $(H_2)_2$ dimer is 0.33 kJ/mol with complete basis sets at MP2 level [11]. Basis sets of low quality might result into too repulsive intermolecular hydrogen potentials. As will be treated later, hydrogen molecules get weakly positively charged upon adsorption to a metal and this increases H_2–H_2 repulsions. An accurate description of H_2–H_2 interactions improves the quality of the results at maximum hydrogen uptake.

3 Physisorption of hydrogen in metals

The crucial aspect is the way hydrogen molecules interact with the adsorbent material, since this physisorptive interaction is the dominant. Precisely the fact that the attractive M-H_2 (with 'M' being the metallic surface or atom) interactions are strong makes possible to overcome H_2–H_2 repulsions and achieve high packing efficiency for storage purposes [12–14]. In MOFs, organic linkers also adsorb hydrogen but only adsorption on the inorganic part is considered here.

The adsorption of hydrogen on transition metals is due to the partly empty d-band of the metal, which gives rise to a high concentration of empty d-levels in the surface, much lower in energy than most of the s-levels. Adsorbed hydrogen becomes weakly positively charged through electronic density transfer from its occupied sigma orbital to the partly empty d-band of the metal. The extent depends on the wavefunctions overlap (according to the M-H_2 orientation and distance) and the energy difference between the orbitals. Figure 1 shows the potential energy curve for a hydrogen molecule in the neighbourhood of a metal [15]. Curve 'a' gives the energy of the chemical bond between two hydrogen atoms and the metal, hence involving a dissociation process, with 'Q' being the heat of chemisorption, corresponding to a strong interaction. Curve 'b' refers to the approach of a hydrogen molecule to the metal and is made up of the attractive London dispersion forces and the usual repulsive forces arising from the interaction of closed electron shells. The value 'q' corresponds to the heat of physisorption, which is a weak interaction. Where the two curves intersect, a molecule held in the physisorbed state may pass into a state of chemisorbed atoms, the necessary activation energy being E_a. The heat of adsorption, in general, decreases with the fraction of metal surface covered, due to the repulsive interaction between adsorbed hydrogen molecules.

Hydrogen adsorption in MOFs presents particular and distinctive features somewhat different than the general remarks above regarding metals. Two particularities of hydrogen adsorption in MOFs are that (1) they do not involve a metallic surface but rather a small inorganic nanocluster containing not only metallic atoms but also a

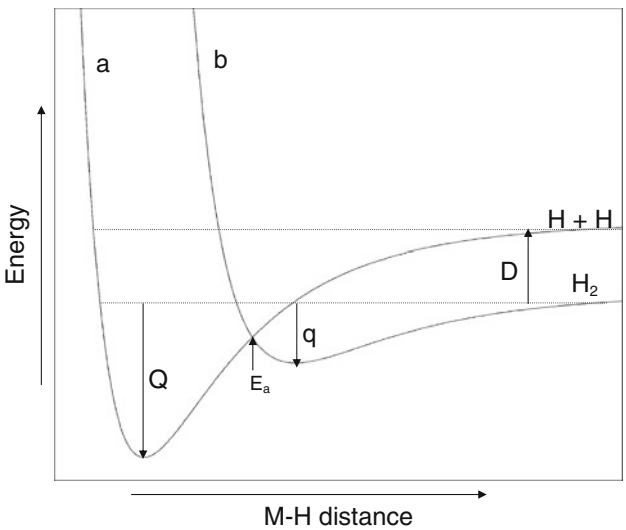

Fig. 1 Interaction of hydrogen with a metallic surface. Curve '*a*': hydrogen is chemisorbed ('*Q*' is the adsorption energy) with dissociation. Curve '*b*': hydrogen is physisorbed, with '*q*' the adsorption energy. A transition from physisorption to chemisorption is possible by applying an activation energy 'E_a'. '*D*' is the dissociation energy of the hydrogen molecule

few atoms (mainly oxygen and also nitrogen) common to the inorganic and the organic parts, and that (2) the metal atoms are therefore partially shielded by the neighbour nonmetallic atoms, this precluding an otherwise larger M-H_2 orbital overlap.

In a schematic manner, the first characteristic of the metal–hydrogen interaction is that electronic transfer (donation, D) occurs between empty spin-orbitals of the metal (M) and the occupied sigma orbital of hydrogen (H_2). A second aspect is an electronic backdonation (BD) which occurs between filled spin-orbitals of the metal (M) and the unoccupied sigma orbital of hydrogen (H_2). Both effects lead to a strengthening of the M-H_2 interaction and a weakening of the H-H bond, and they, overall, produce a net electronic transfer from the hydrogen (H_2) to the metal ('D' from hydrogen to metal and 'BD' from metal to hydrogen). The extent of electronic transfer will depend on the relative energies of the orbitals involved in the electronic transfer as well as their overlap. This interaction becomes particularly strong in Kubas-type complexes [16], where the hydrogen molecule acts as a ligand, but this is never the case in MOFs, except when open metal sites are available. In general, MOFs contain metals with the organic ligands fully coordinated and therefore metals do not offer coordination vacancies to the hydrogen molecules. Backdonation can be enhanced by the use of electrodonating organic ligands which make the metal richer in electronic density. Conversely, donation can be activated when the organic ligands are electronic acceptors. These two electronic transfer mechanisms (D and BD) are possible because of the amphoteric character of the hydrogen molecule which can behave both as a Lewis acid and base with respect to metals.

A third contribution and mechanism of M-H_2 interaction is the purely electrostatic which can be (1) charge-quadrupole (proportional to R^{-3}) taking into account that H_2 is a molecule with quadrupole moment, or (2) charge-induced dipole (proportional to R^{-4}) provided the metal is sufficiently charged so as to generate an induced dipole in the hydrogen molecule. Both interactions depend strongly on the net charge of the metal, which in turn depends on the metal atom and the Lewis acid–base character of the organic ligands. In the weakest case, when no significant net charge is present in the metal, the interactions are (3) induced dipole-induced dipole, or dispersive (van der Waals or London type of interactions, proportional to R^{-6}) [17].

The relative importance of these three main contributions to M-H_2 interactions in MOFs can be estimated through energy decomposition schemes [16]. Although we are only considering the interaction as M-H_2, MOFs contain atoms covalently bonded to the metal, which also interact with hydrogen.

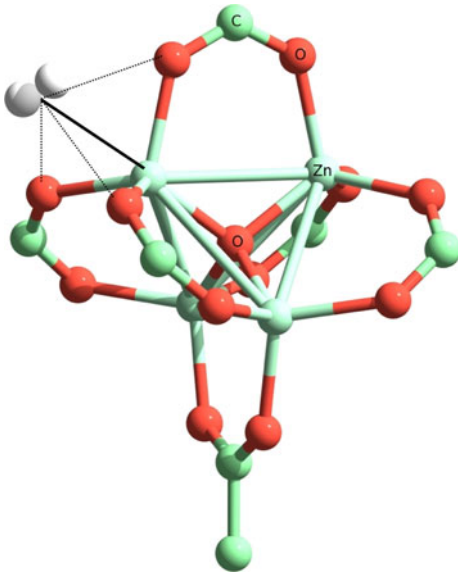

Fig. 2 Interaction between a hydrogen molecule and a metallic cluster from the IRMOF series. The hydrogen molecule interacts with a metal atom (tetrahedron vertex) and its three adjacent oxygen atoms. The distances highlighted are approximately 2.4 Å

4 Topological features of the hydrogen-MOF interactions

The hydrogen molecule does not only interact with metal atoms but also with oxygen (or nitrogen) atoms belonging to the inorganic nanocluster. Figure 2 corresponds to the inorganic cluster of the so-called iso-reticular series of MOFs (also called IRMOFs, with IRMOF-1 being the archetypal MOF-5) and can be taken as a general case to illustrate that the metal–hydrogen interaction is shielded by atoms of the inorganic nanocluster, in this particular case oxygen atoms from a dicarboxylate group. Apart from the M-H_2 interactions, O-H_2 should also be playing an important role, and this will depend on the topology and geometry of the framework which defines the accessibility of the incoming hydrogen molecules [18]. If we look at PCN-9 [19] structure (Fig. 3), it can be appreciated how the different connectivity of the metal cluster and the organic ligand results in a different accessibility and interactions from the hydrogen molecule to the metal and the oxygen atoms. The large variety of metal cluster topologies in metal–organic frameworks makes a daunting task to systematise all the possible cases although some efforts, for example by the group of O'Keeffe, have been made [20–22]. Far from such systematisation, the cases presented in Figs. 2 and 3 can be taken as two extreme cases where the metal is shielded (Fig. 2) and unshielded (Fig. 3) by nonmetallic atoms. In a qualitatively sense, these two cases may represent physisorption and chemisorption of hydrogen, respectively. Most of the interactions

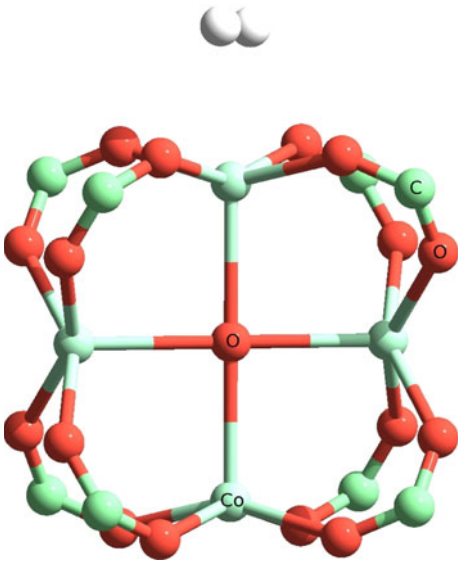

Fig. 3 Interaction between a hydrogen molecule and a metal–organic framework, PCN-9 [19], containing open metal sites. A fragment of the inorganic cluster of PCN-9 is shown where there is a square-planar $Co_4(\mu_4\text{-O})$ unit with a μ_4-oxo at the centre of a square of four Co atoms. All four Co atoms in the unit are five-coordinated with square pyramidal geometry. The Co-μ_4-O distance is 2.35 Å

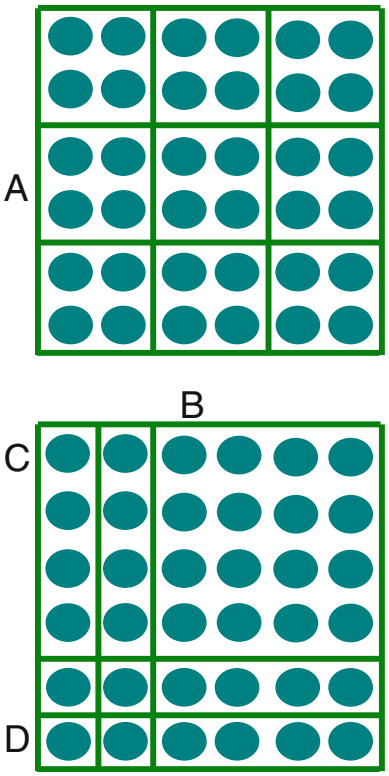

Fig. 4 Effect of the pore size distribution on the adsorption of hydrogen molecules (*ellipses*) in a porous surface. *Top figure* a uniform pore size (*A*). *Bottom figure* different pore sizes ($B > C > D$) which will be associated with different adsorption energies. Two types of adsorption centres appear for the hydrogen molecules in *C*, which are in contact to either two or three surfaces. Three types of adsorption centres appear for the hydrogen molecules in *B*, which are in contact to either none, one, or two surfaces. The specific surface of the material is the same in both cases (*top* and *bottom*)

correspond to the first case (Fig. 2) and therefore physisorption applies, with interactions between 1–10 kJ/mol; but stronger interactions are at play in frameworks with open metal sites (also called 'coordinatively unsaturated metal centres') (Fig. 3), involving interactions that can be larger than 10 kJ/mol.

A question related to the convenience or not of open metal sites is the relation between connectivity (topology) and porosity. Open metal sites clearly provide a stronger interaction but, does the presence of open metal sites limit the specific surface or the volumetric capacity of the material?. Open metal sites (coordinatively unsaturated metal atoms) imply a relatively void region of the material, and this is related to larger porosity.

Porosity and specific surface are interrelated parameters which depend on the topology of the network (See the excellent discussion in paragraph 3.2 of ref. [7], and also ref. [23]). Figure 4 shows a simple scheme which illustrates how different pore size distributions can be achieved with materials of equal specific surface. Hydrogen molecules may have uniform adsorption centres with equal energies (Fig. 4, top), or there can be different adsorption sites according to the environment (Fig. 4, bottom). The adsorption energetics are expected to be influenced by the pore size and hence confinement effects appear when the adsorbate interacts also with the opposite part of the pore wall (Fig. 4, pores C and D) [24]. Another important possibility is shown by the pore type B (Fig. 4, bottom), where some of the hydrogen molecules are not in contact with the MOF surface. These molecules are not expected to have a strong energetic interaction with the material and they remain occluded as an effect of the pressure applied.

The above picture considers the interaction of only one hydrogen molecule per metallic centre, but metallic centres have the ability to adsorb several hydrogen molecules with loading affecting the isosteric heat of adsorption. Hydrogen storage requires the interaction of as high as possible number of hydrogen molecules per metallic atom. The number of hydrogen molecules that can interact with each metallic atom is directly related to the topology of the MOF. An example is seen in Fig. 5, which shows hydrogen adsorbed at an inorganic cluster characteristic of the IRMOF series of materials [18].

How is the adsorption energy affected by increasing hydrogen loading?. It is expected that H_2–H_2 interactions should contribute to decrease the adsorption energy. Hence, we now consider more in detail adsorption energies, and the relation with loading, pressure and temperature.

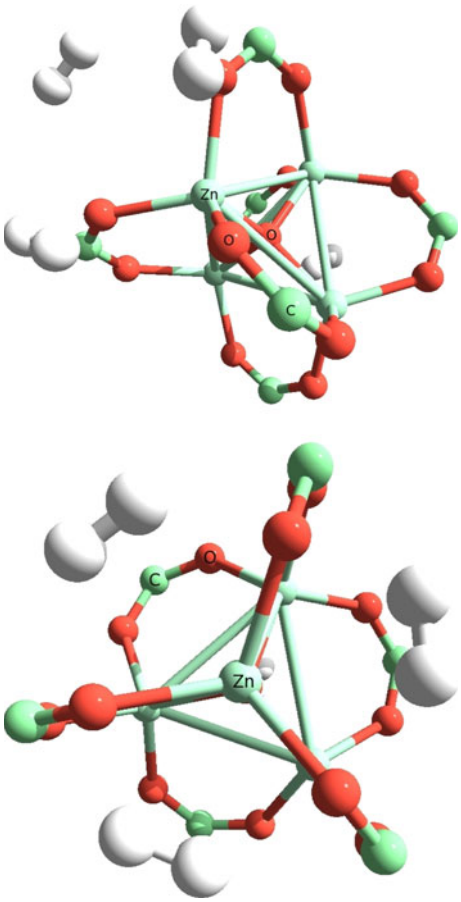

Fig. 5 Two perspective views (*top* and *bottom*) of four hydrogen molecules adsorbed at the inorganic cluster corresponding to IRMOF structures. Three hydrogen molecules interact with a metal atom at the vertex of a tetrahedra, and one hydrogen molecule interacts at the face of the tetrahedra. At full coverage (4 vertex, 4 faces), 16 hydrogen molecules can be adsorbed in this metallic cluster [41]

5 Energetics of the physisorption of hydrogen in MOFs

Previous studies including atomistic treatments have allowed to estimate accurately adsorption isotherms of hydrogen in MOF-5. Garberoglio et al. [25] made a remarkable effort to ensure a correct treatment of the intermolecular $H_2 \cdots H_2$ interactions, based on the Darkrim and Levesque forcefield [26], which allows to reproduce reasonable well the density of hydrogen at different pressures and temperatures. Their study [25], based on a Monte Carlo approach, 'switches' on and off the effect of the charges to the adsorption and this provides valuable estimates of the contribution of the electrostatic part to the adsorption process. Also, an estimate of the volume density of states was possible, which is very useful in order to assess storage capacities.

Using a similar Monte Carlo–based methodology, Snurr et al. [27, 28], obtain reasonably good estimates of the excess adsorption and maximum uptakes at different temperatures (77 and 298 K) on a wide range of materials and correlate the results with isosteric heats of adsorption and pore size. More details about hydrogen storage in MOFs using atomistic approaches can be found in a recent review [10].

Sophisticated quantum chemical treatments allow to estimate accurately physisorption of hydrogen in MOFs. Experimental values suggest energy values for the interaction of hydrogen with metal–organic framework within the range of 1–10 kJ/mol, and larger than 10 kJ/mol if open metal sites are available in the material [7]. An accurate estimation of these energetics requires a careful use of the quantum chemistry approaches available in the literature.

Long-range interactions, such as those involved in physisorption, are poorly described in most of the presently available exchange–correlation functionals within Density Functional Theory (DFT). Approximations to calculate the exchange and correlation energies are divided into two main categories. The local density approximation (LDA) assumes that the exchange and correlation energies are a function of the electron density at the point of evaluation. The generalised gradient approximation (GGA) takes into account the gradient of the electron density at the point of evaluation. LDA has a tendency to overestimate the binding energies between two molecules, compared with experimental results, whereas GGA—in general—tends to underestimate binding energies predicting a shallow or flat adsorption well. In some cases, particular functionals have given good agreement with experimental results through fortuitous error cancellations between exchange and correlation energy approximations. It is known, however, that no DFT functional accurately describes all the characteristics of molecular interactions, in particular van der Waals (London dispersion) interactions, which are, in part, due to electronic correlation.

In Hartree–Fock methods, correlation can be taken into account through post-treatments such as second-order Møller–Plesset (MP2) perturbation theory. In order to obtain sufficiently accurate results, high-quality basis sets (such as 6-31G(d), cc-pVDZ, or equivalent) as well as corrections due to basis set superposition error (BSSE) should be considered. Without diffuse functions, the BSSE can amount up to 50% of the adsorption energy.

Most of the quantum chemistry studies have been carried out on MOF-5 due to the wealth of experimental results available in the literature to compare with and that is why it is convenient to analyse quantum chemistry studies on MOF-5 (see Table 1).

Plane waves and the local density approximations (LDA), as well as neutron diffraction, were used to study hydrogen adsorption in MOF-5 by Yildirim and Hartman [29], who found that at low pressure and very low temperature (3.5 K) hydrogen is mainly adsorbed at the

Table 1 Calculated adsorption energy (kJ/mol) of a single hydrogen molecule in MOF-5

Ref	E_{ads}	Site[a]	Model[b]	Method[c]
29	−15.4	Face	Periodic	LDA/PW/US-PP
	−11.1	Vertex	Periodic	LDA/PW/US-PP
32	−9.2	Vertex	cl + H	MP2/TZVP
	−6.9	Vertex	cl + H	CBS
31	−6.3	Vertex	cl + H	RI-MP2/QZVPP
33	−15.4	Face	Periodic	LDA/PW/PAW
	−10.2	Vertex	Periodic	LDA/PW/PAW
34	−6.8	Face	Periodic	GGA/PW/US-PP
	−6.8	Vertex	Periodic	GGA/PW/US-PP
35	−2.3	η^2-O	cl + H	MP2/BSSE, optimised cluster[d]
	−3.2	η^2-O	cl + H	MP2/BSSE, single point[e]
	−0.7	Vertex	cl + H	MP2/BSSE, optimised cluster[d]
	−2.0	Vertex	cl + H	MP2/BSSE, single point[e]
37	−2.7	Face	cl + H	PW91/6-311 ++G**/BSSE
	−2.0	Vertex	cl + H	PW91/6-311 ++G**/BSSE
38	−3.1	Face	cl + H	PBE/MP2/TZVPP/BSSE
	−1.0	Vertex	cl + H	PBE/MP2/TZVPP/BSSE
	−1.1	Face	cl + benzene	PBE/TZVPP/BSSE
	−2.1	Vertex	cl + benzene	PBE/TZVPP/BSSE
40	−5.1	Face	cl + H	Optimisation + single point[f]
	−3.1	Vertex	cl + H	Optimisation + single point[f]
44	−4.1	Face	cl + H	MP2/aug-cc-pVTZ/BSSE, single point[g]
	−1.7	Vertex	cl + H	MP2/aug-cc-pVTZ/BSSE, single point[g]
	−5.9	Face	cl + benzene	MP2/aug-cc-pVTZ/BSSE, single point[g]
	−3.8	Vertex	cl + benzene	MP2/aug-cc-pVTZ/BSSE, single point[g]
	−5.4	Vertex	cl + H	MP2/aug-cc-pVTZ/BSSE, optimised cluster
	−5.8	Vertex	cl + H	MP2/aug-cc-pVQZ/BSSE, optimised cluster
	−6.0	Vertex	cl + H	MP2/CBS/BSSE, optimised cluster

[a] 'face' and 'vertex' sites as indicated in Fig. 5. Sites are also called: β and ZnO_3 (vertex); α and 'cup site' (face). η^2-O: see reference

[b] cl + H: cluster of Fig. 2 terminated by H; cl + benzene: cluster of Fig. 2 terminated by benzene

[c] PW: plane waves; US-PP: ultra-soft pesudopotentials; CBS: complete basis set. For the other acronyms see text

[d] basis set: 6-311 ++G** (H), 6-31 + G** (C,O), Lanl2DZ (Zn)

[e] basis set: aug-cc-pVQZ (H), 6-31 + G** (C,O), Lanl2DZ (Zn)

[f] geometry otimisation: B3LYP/6-31G(d); and energies calculated as single point with: aug-cc-pVQZ (interacting atoms) and 6-31 + G(2d,p) (farther atoms). See more details in reference

[g] Structure taken from a periodic DFT/PBE (constant volume) optimisation. The loading here is 4 hydrogen molecules per unit cell

metallic cluster, with the organic ligand playing a secondary role. They report calculated adsorption energies between −11 and −15 kJ/mol for a single hydrogen molecule adsorbed at the different sites.

When comparing computational and experimental adsorption energies, the effect of loading should be taken into account. Rowsell and Yaghi [30] report isosteric heats of adsorption between 4 and 5 kJ/mol for hydrogen in MOF-5 throughout the range of loading considered. This was determined from the adsorption isotherms by using a fit based on a virial-type equation relating pressure, temperature and hydrogen amount adsorbed.

Sagara et al. [31] use a high-quality RI-MP2 (resolution identity and second-order Møller-Plesset) with TZVPP (triple-zeta-valence augmented with three sets of polarisation functions for main group elements and two for transition metals) basis set to optimise a metallic cluster within the isostructural IRMOF series, and then perform a single-point energy calculation with QZVPP basis, and find a binding energy of 6.3 kJ/mol for a single hydrogen molecule, without reporting the equilibrium geometry. In a similar study [32] they give values of −6.9 and −9.2 kJ/mol. Their calculations show that organic linkers with appropriate characteristics show a weaker adsorption

strength than the metallic centre. The methodology used includes a treatment of the correlation energy with dispersion forces, which are excluded by other methods such as most DFT approaches and which are important in weakly binding systems as the one considered.

Samanta et al. [33] use the projector augmented-wave (PAW) method within the plane-waves methodology and the local density approach and find a hydrogen adsorption energy in MOF-5 between −10 and −15 kJ/mol at low coverage. This is in agreement with Yildirim and Hartman [29], due to the use of the same methodology, and the authors estimate—as mentioned above—that this methodology gives an overbinding on these type of materials by an approximate factor of 2, due to the fact that the LDA approximation cannot give accurate values of the dispersion interactions when there is significant overlap of electron densities. The authors point that other functionals such as PBE and PW91, based on GGA (generalised gradient approximation), are expected to perform worse than LDA at intermediate ranges of weak interactions, but this claim is not demonstrated. The authors also explain that effects related to the changes in zero-point vibrational energy of the hydrogen molecule upon adsorption can be safely neglected based on Raman spectroscopy experiments which estimate this effect on the range of less than 0.1 kJ/mol.

Mulder et al. [34] carry out plane-wave calculations within a GGA approach on MOF-5 and find that the strongest adsorption sites are located in the metallic cluster where an interaction of hydrogen occurs mainly with O and Zn atoms. They found an adsorption energy about −6.8 kJ/mol at low coverage, which compares reasonably well, according to the authors, to the values obtained from inelastic neutron scattering experiments, which measure the energy shift of the rotational transition $J = 0 \rightarrow 1$ of hydrogen adsorbed with respect to free hydrogen.

Bordiga et al. [35] performed IR experiments to measure the red-shift of the hydrogen stretching frequency upon adsorption, as well as ab initio calculations on hydrogen adsorption at clusters of MOF-5 including high-quality basis sets at the MP2 level with BSSE corrections. Two adsorption geometries, strictly identical to those considered in Fig. 5 (vertex and face), were denoted by the authors as η^2-Zn and η^2-O and the respective calculated adsorption energies were −2.0 and −3.2 kJ/mol, respectively, with the surprising geometric result that the hydrogen-Zn and hydrogen-O distances were 3.18 and 4.43 Å, respectively (the larger distance corresponds to the stronger adsorption). In both cases, H–H bond elongation is observed, as expected, with the respective values 0.001 and 0.003 Å. It is highlighted that in both cases, the hydrogen molecule interacts with more atoms, apart from the closest, so in both cases Zn and O atoms are involved in the physisorption. The authors fail to note that in the η^2-Zn interaction, the geometry of the neighbour O atoms precludes the hydrogen molecule to interact more strongly with the Zn atom. Our argument (see Fig. 2) is that even in the most favourable case of H_2–Zn interaction, when only one hydrogen molecule attacks the Zn atom adopting an adsorbed conformation of the type η^2-Zn, the neighbour O atoms are also close to the hydrogen molecule, precluding an otherwise shorter H_2–Zn distance. This is also the case at higher loadings, when several hydrogen molecules physisorb near each Zn atom (Fig. 5), and therefore H_2–O interactions are very important in the case of η^2-Zn adsorption. Dissociative hydrogen chemisorption would be observed if the O atoms were not shielding the H_2–Zn interaction, as it is the case in materials where Zn is exposed [36].

Negri and Saendig [37] investigate hydrogen adsorption in an IRMOF-type metallic cluster using a cluster model and a DFT methodology with the PW91 functional and 6-311++G** basis set including the BSSE correction. PW91 and PBE are the two GGA-type functionals that give better results for weakly bound systems because they are free from some of the repulsive contributions (both functionals satisfy the Lieb-Oxford bound) that make other GGA functionals unable to capture weak interactions. Energies of −2.0 and −2.7 kJ/mol are found for the η^2-Zn and η^2-O interactions, respectively, at low coverage, with the corresponding H–Zn and H–O distances being 3.42 and 4.05 Å.

Klontzas et al. [38] employ different cluster models of IRMOFs to study how the calculated results of hydrogen adsorption depend on the model used and they conclude that the model size affects the polar behaviour of the metal site, which in turn has an influence on the adsorption energy. Cluster models terminated by hydrogens and by benzene groups show adsorption energies of −2.9 and −1.1 kJ/mol, respectively, at the metal-face site as calculated from DFT method with PBE (GGA) functional, TZVPP basis set, counterpoise corrected BSSE, but without MP2 corrections. An equivalent calculation with MP2 corrections on a small cluster terminated by hydrogens gives the adsorption energy of –3.1 kJ/mol. It is estimated that BSSE can account for up to 50% of the binding energy and hence it is a very important correction. Adsorption at other sites is slightly less favourable. The study does not take into account the effect of loading as only the interaction of one hydrogen molecule has been considered.

Some of the referred computational studies regarding hydrogen physisorption on the metallic cluster of IRMOFs conclude that the metal site (and hence the η^2-Zn) interaction is weaker than the interaction with the carboxylic oxygen atoms (η^2-O), and even some experimental interpretations are quoted to justify this result. This is a counter-intuitive result since metals rather than oxygens

are supposed to be the atoms with the larger capacity to adsorb hydrogen, as explained in previous sections. It seems more reasonable—and some computational results indicate—so that it is the η^2-Zn interaction which dominates the sorption at low coverage, as suggested from the experimental results by Rowsell et al. [39]. Nevertheless, this is an open question subject to debate. As for the dominant nature of the interactions, except in the case of strong polarisation of charged metals into the hydrogen molecule (charge-induced dipole), the London dispersion forces seem to be the dominant in the physisorption of hydrogen in metal–organic frameworks, with also some contribution (depending on the metal charge) from induced dipole–dipole interactions. Few quantum chemistry studies at very high level have been performed so far, and many kinds of metallic clusters present in MOFs have yet to be properly modelled in order to update our knowledge on this topic. From the computational studies revised, MP2 calculations with large basis sets and BSSE corrections seem of the quality necessary to give an accurate account of these weak interactions. The study by Kuc et al. [40] employs such methodology with a complete comparative study of the effect of different basis sets of high quality. Results with the base aug-cc-pVQZ for the strongly interacting atoms in a small cluster give an adsorption energy of −4.2 kJ/mol for the η^2-Zn interaction with a H–Zn distance of 2.9 Å. When a larger cluster—and a smaller basis set—is used, a comparison between the η^2-Zn (vertex site) interaction and the face-type geometries (see Fig. 5) gives energies of −3.1 and −5.1 kJ/mol, and distances (to the closest atom) 3.1 and 3.7 Å, respectively.

Gomez et al. [41] use a similar methodology than that previously described [40], and a larger cluster, but focusing on the effect of incoming H_2 molecules on the energetics of the adsorption process. The maximum uptake correspond to 3 hydrogen molecules at each vertex site and 1 hydrogen molecule at each face site, resulting in 16 hydrogen molecules per tetrahedral cluster unit (Fig. 5), which results in a ca. 4% weight capacity, in good agreement with an experimental accurate estimation of 4.5–5.2% [42]. Adsorption energies were calculated through ab initio methods including large basis sets, 6-31++G(d,p), correlation effects at the MP2 level and including BSSE corrections, giving a value, at high loading, of −2.4 kJ/mol. This is lower binding than a recent experimental determination of −4.1 kJ/mol [43].

Sillar et al. [44] also use a similar methodology and cluster model [40, 41], considering 4 H_2 molecules per metallic cluster, and include zero-point vibrational energy corrections, obtaining adsorption energies of −4.1 and −1.7 kJ/mol for the face and vertex sites, which they call 'α' and 'β', respectively, using a small cluster. Enlarging the cluster—considering the benzene rings—and with a different geometry optimisation strategy, the values are −5.9 and −3.8 kJ/mol, respectively.

Fu and Sun [45] also use the small cluster (also called 'formiate model') with a sophisticated methodology based on RI-MP2 and TZVPP basis set including BSSE corrections and find that the adsorption energies are −5.4 and −2.5 kJ/mol for the sites 'face' and 'vertex', respectively, in close agreement with the study by Sillar et al. [44]. Only calculating the adsorption energy in the 'face' centre, with a very similar methodology, Han and Goddard [46] found a value of −6.2 kJ/mol, which shows again an overall agreement with all the studies carried out with a high-level methodology based on MP2 post-HF treatment, large basis set and BSSE corrections.

The 'resolution of the identity' integral approximation applied to second-order many-body perturbation theory (RI-MP2) introduces a new auxiliary basis set into the method and offers improved computational performance compared to exact MP2 calculations at a very small cost in terms of accuracy. Sillar et al. [44], among others mentioned above, employ this method whose efficiency allows to increase substantially the cluster size and include benzene rings to model a larger part of the MOF-5 structure. Although benzene rings do not pose a steric constraint to the hydrogen adsorption, they do contribute to the electronic redistribution at the zinc and surrounding atoms, and hence affect adsorption energies: compare for example the values −4.1 (small cluster) and −5.9 kJ/mol (large cluster) in Table 1 (MP2/aug-cc-pVTZ). According to this, neglecting the organic part to consider hydrogen adsorption in MOFs does not only lead to the obvious conclusion of missing adsorption at the organic linkers, but also to the synergistic effect that the organic makes into the inorganic nanocluster through electronic redistribution effects. This has been treated in detail elsewhere [47, 48].

Systems other than MOF-5 and the other IRMOFs have also been investigated but fewer studies are available, of which we extract a selection in Table 2. In particular, and to recall information on hydrogen adsorption in MOFs containing exposed metal sites, a system studied both experimentally and quantum chemically is a material (see Fig. 6) based on the BTT^{3-} (1,3,5-benzenetristetrazolate) organic linker [49]. This is a complex structure in which electrostatic interactions play an important role due to the charged nature of the framework, consisting of chloride-centred square-planar $[Mn_4Cl]^{7+}$ units linked to the tri-negative ligands to give a $[(Mn_4Cl)_3BTT_8]^{3-}$ framework, compensated by extraframework $[Mn(CH_3OH)_6]^{2+}$ cations in the relative proportions 2:3. The metallic cluster and the position for hydrogen adsorption (as determined from neutron powder diffraction) at low coverage are shown in Fig. 6. The measurements give H_2–Mn distance 2.27 Å and

Table 2 Calculated and experimental adsorption energies (kJ/mol) of hydrogen on selected materials

E_{ads}(calc)	ΔH_{ads}(exp)	Material
−8.4 [50]	−10.1 [49]	$[Mn(CH_3OH)_6]_3[(Mn_4Cl)_3BTT_8]_2$
−13.3 [51]		
−23.8 [52]		Ni[CH3OCH3]3[OCH3]2
−7.3 [54]	−13.5 [55]	CPO-27-Ni
−9.6 [58]	−8.8 [57]	MOF-74
−28.9 [59]	−10.1 [55]	HKUST-1

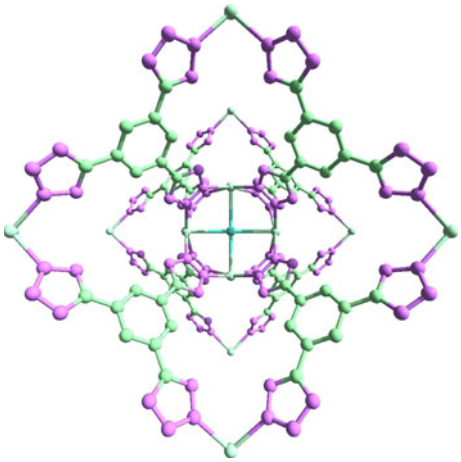

Fig. 6 Perspective view of the metallic cluster of the Mn-BTT metal–organic framework [49] (hydrogen atoms omitted for clarity). The central part contains a $[Mn_4Cl]^{7+}$ cation with the Mn atoms showing a square-planar geometry. In the direction perpendicularly to such plane, inwards, there is the chlorine anion, and outwards is the location where hydrogen molecules preferentially adsorb

an isosteric heat of adsorption of −10.1 kJ/mol. Plane-wave calculations by Sun et al. [50] with the PBE functional gave 2.42 Å H_2–Mn distance and an adsorption energy of −8.4 kJ/mol when taking into account the ferromagnetic configuration of the Mn atoms. Later, work by Zhou and Yildirim [51] with the same methodology indicates that the ground state is not ferromagnetic but of a dimer type between the four Mn atoms (two spins are antiparallel to the other two). The authors also found that the spin state of each Mn atom rather than the magnetic configuration has a more important effect in the adsorption energy, with the high-spin state showing an adsorption energy of −13.3 kJ/mol, considerably larger than that of the low-spin state which is −8.1 kJ/mol. This study includes rotational corrections on the adsorbed hydrogen at 77 K, which is not expected to be in its fundamental rotational state. The authors estimate this effect, in this case, to reduce binding in about 30% of the adsorption energy.

An interesting study was presented by Kosa et al. [52] where square pyramidal Ni_2+ organometallic complexes, $Ni[CH_3OCH_3]_3[OCH_3]_2$, potentially inorganic building units of MOFs, showed a strong covalent interaction with hydrogen involving electronic transfer HOMO(H_2)→LUMO(Ni-complex) and HOMO(Ni-complex)→LUMO(H_2). The optimisations were carried out at the BLYP/6-311G(d) level of theory with BSSE corrections and a maximum adsorption energy of −23.8 kJ/mol was found. Changing the charged ligand (−OCH_3) locations from 'cis' to 'trans' and to 'axial' had a remarkable effect on the adsorption energies which ranged between −6.4 and −23.8 kJ/mol. This shows that although adsorption may be dominated by the metallic part, the organic ligands make an important contribution to the adsorption energy through changes in the electronic density at the metal site.

An interest on MOFs containing Ni led recently to the synthesis of CPO-27-Ni [53], where also a square pyramid coordination for Ni is found. The hydrogen adsorption was calculated by Zhou et al. [54] using GGA (PBE exchange–correlation) and LDA (Perdew-Zunger exchange–correlation) functionals within a plane-wave methodology using Vanderbilt ultra-soft pseudopotentials. The respective energies were −7.3 and −39.0 kJ/mol. Although GGA functionals are not adequate for dispersion interactions, in this case electrostatic and charge transfer are the dominant interactions, which are more accurately calculated by this methodology, and thus the GGA value of −7.3 kJ/mol should be taken as a more reasonable approximation than the LDA result. A variable temperature infrared (VTIR) study gives an adsorption enthalpy of −13.5 kJ/mol [55], which makes this one of the strongest hydrogen adsorption sites found in MOFs. Unfortunately, CPO-27-Ni does not contain sufficient density of centres and the maximum uptake is not larger than 2% at 77 K and 45 bar [55]. To this low uptake also contributes the high density (and low specific surface) of the material.

Isostructural to CPO-27-Ni is MOF-74, containing Zn instead of Ni, whose hydrogen uptake at saturation is 2.3% at 77 K and 26 bar [56]. Neutron diffraction and inelastic neutron scattering experiments show that adsorption enthalpies range between −8.8 and −4.0 kJ/mol at low and high loading, respectively [57]. An accurate first-principles study [58] has been done at the periodic DFT level using the vdW-DF methodology which incorporates the van der Waals interactions, traditionally underestimated in most functionals, into a fully nonlocal and nonempirical treatment of the correlation energy, which retains the ordinary good DFT performance in describing covalent bonding. Vibrational zero potential energy corrections have also been taken into account and an adsorption energy of −9.6 kJ/mol was found, in close agreement with the above experimental results.

Along the lines of searching large adsorption energies together with sufficiently large specific area and adequate

pore volume, another interesting material is HKUST-1 whose approximate Langmuir specific area is $\sim$2,300 m^2/g, larger than that of MOF-74 ($\sim$1,150 m^2/g) [56]. HKUST-1 contains a paddle-wheel topology for the inorganic building unit and the metal is Cu. Due to the accessibility of the metal sites and the large area, HKUST-1 adsorbs 3.2% hydrogen at 77 K and 50 atm [8]. A recent first-principles study [59] using a periodic DFT plane-wave methodology and Vanderbilt ultra-soft pseudopotentials, with an energy cut-off of 408 eV and keeping the cell parameters fixed to the experimental value find an adsorption energy of -28.9 kJ/mol, far too high. The experimental VTIR determination by Vitillo et al. [55] gives a value of -10.1 kJ/mol for the adsorption enthalpy.

It is clear that not only a sufficiently large adsorption energy is necessary but also a large specific area and a low density. Increasing the adsorption energy through the presence of coordinatively unsaturated metal sites usually leads to a decrease in the surface area and an optimum compromise which gives a large hydrogen uptake (ca. 6%) at moderate P,T conditions has yet to be achieved in order to reach commercial targets.

6 Characterisation of hydrogen uptake in MOFs

From the points above, it becomes clear that an appropriate balance between number (per volume unit) and strength of centres is required and both parameters can be experimentally measured. Two important methods to characterise hydrogen uptake are gravimetric and volumetric, where uptake is typically characterised by adsorption isotherms measured at 77 K and pressures between 1–100 atm. The accuracy of the results is an issue [42], especially when gravimetric methods are used, taking into account the low molecular weight of hydrogen, its purity and leaks derived from its high diffusivity. The data are normally fit to either Langmuir or BET models which consider one or two values for the heats of adsorption within a monolayer or multilayer approximation, respectively. By considering data at different temperatures and applying the Clausius-Clapeyron equation, the isosteric (constant coverage) heat of adsorption can be obtained. A sufficiently large isosteric heat of adsorption (leading to a steep rise in the adsorption isotherm in the low pressure range) and a large saturation capacity are the two necessary conditions for storage applications (Fig. 7). Large (small) heats of adsorptions correspond to a fast (slow) rise in the mass of hydrogen adsorbed at low coverage (pressures). The final saturation capacity indicates the total capacity of the material, which is related to its specific surface area.

Too large heats of adsorption are of no use in storage applications, giving slow desorption kinetics and excessive

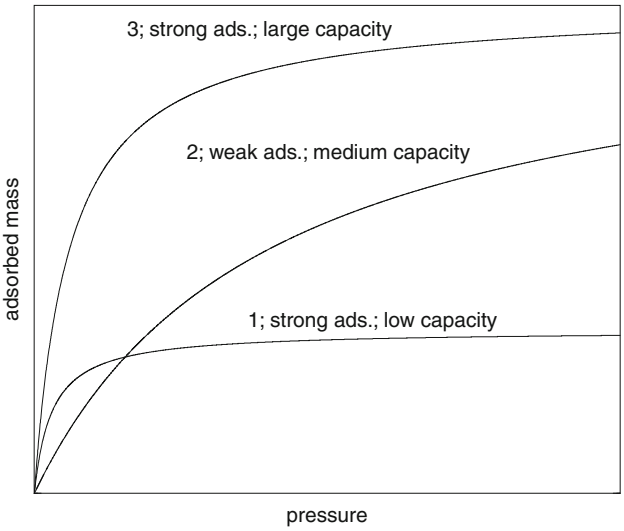

Fig. 7 Schematic representation of three Langmuir isotherms of hydrogen adsorption in different types of metal–organic frameworks. *Curve 1*: the material contains few and strong adsorption sites. *Curve 2*: the material contains more adsorption albeit weak centres. *Curve 3*: the material contains many and strong adsorption sites

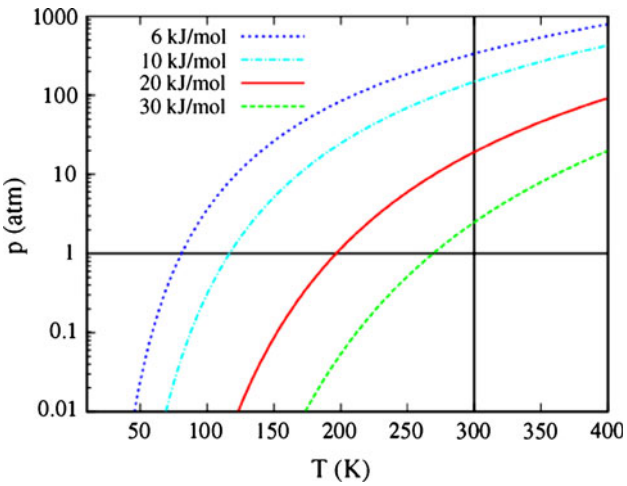

Fig. 8 Equilibrium pressures of hydrogen adsorption on surfaces plotted as a function of temperature using van't Hoff equation for several binding energies. Taken from reference [60]. Reproduced with permission from Elsevier

heating; therefore an optimum heat of adsorption is needed. The work by Jhi [60] shows a plot of the equilibrium pressures of hydrogen adsorption on surfaces as a function of temperature using the van't Hoff equation for several binding energies, with the results shown in Fig. 8. From the plot, for example, desorption at room temperature and pressure in the range 1–10 atm requires binding energies of about 30 kJ/mol. Relaxing the conditions for adsorption/desorption at room temperature and 10–100 atm, still within commercial constraints, binding energies between 10–20 kJ/mol are necessary. The latter values are not too far from what has been shown in some MOFs above, but

such materials do not yet meet the other essential requirement of a sufficiently large specific area. In spite of the progress made, still larger improvements are required for the commercial use of MOFs in hydrogen storage. We believe that quantum chemistry calculations are an invaluable aid to guide further research in this area.

7 Conclusions and prospects

Hydrogen storage for commercial applications is one of the bottlenecks for the realisation of a global scale hydrogen economy. Targets to achieve commercial success by using metal–organic frameworks as physisorbents are still far from the present-day results. Most of the quantum chemistry studies have been based on the IRMOF series (specially MOF-5) due to the large experimental available data to compare with. Confident experimental data for MOF-5 indicate a saturation capacity of ca. 5% [42] and an isosteric heat of adsorption, at low loading, of −5 kJ/mol [30]. The results considered on MOF-5 (Table 1) show that accurate models and methodologies are able to reproduce the experimental result of both adsorption energy and maximum uptake. From the computational studies, a few conclusions can be drawn: (1) models require a minimum size as that in Fig. 2 which, nevertheless, neglects the electron transfer effects between the organic ligand and the metallic cluster; (2) hydrogen physisorption is dominated by very weak dispersion forces and hence electronic correlation becomes important. For Hartree–Fock methods a treatment at the MP2 level is appropriate, but the basis set dependence should be checked. Large basis sets (such as 6-31G(d), PVTZ, cc-pVTZ, or equivalent) as well as corrections due to basis set superposition error should be considered. New DFT functionals where an improved description of the long-range dispersion interactions is included [61] are a promising area of further research. Current GGA functionals, such as PW91 or PBE, seem to perform reasonably well, while LDA functionals seem not appropriate for the treatment of systems dominated by London dispersion forces.

MOF materials, where stronger physisorption than that on MOF-5, are required for storage applications and a few have already been proposed. Estimations indicate that commercial applications need no less than 10 kJ/mol adsorption strengths as well as saturation weight uptakes clearly larger than 5%. Quantum chemistry studies on MOF materials show these targets are not met in current MOFs. Ways to improve the adsorption such as new inorganic cluster types and appropriate pore size are among the topics that are currently being developed. The system models require an accurate description so as to take into account the effects of high hydrogen loadings thus mimicking the real material as much as possible.

Acknowledgments The author thanks Ministerio de Ciencia e Innovacion of Spain for funding through project MAT2007-64682.

References

1. Kitagawa S, Uemura K (2005) Dynamic porous properties of coordination polymers inspired by hydrogen bonds. Chem Soc Rev 34:109–119
2. Yaghi OM, O'Keeffe M, Ockwig NW, Chae HK, Eddaoudi M, Kim J (2003) Reticular synthesis and the design of new materials. Nature 423:705–714
3. Rosseinsky MJ (2004) Recent developments in metal-organic framework chemistry: design, discovery, permanent porosity and flexibility. Micropor Mesopor Mater 73:15–30
4. Férey G (2008) Hybrid porous solids: past, present, future. Chem Soc Rev 37:191–214
5. van den Berg AWC, Otero-Areán C (2008) Materials for hydrogen storage: current research trends and perspectives. Chem Commun 668–681
6. Lin X, Jia J, Hubberstey P, Schröder M, Champness NR (2007) Hydrogen storage in metal-organic frameworks. Cryst Eng Comm 9:438–448
7. Zhao D, Yuan D, Zhou H-C (2008) The current status of hydrogen storage in metal-organic frameworks. Energy Environ Sci 1:222–235
8. Rowsell JLC, Yaghi OM (2005) Strategies for hydrogen storage in metal-organic frameworks. Angew Chem Int Ed 44:4670–4679
9. Keskin S, Liu J, Rankim RB, Johnson JK, Sholl DS (2009) Progress, opportunities, and challenges for applying atomically detailed modelling to molecular adsorption and transport in metal-organic framework material. Ind Eng Chem Res 48:2355–2371
10. Düren T, Bae Y-S, Snurr RQ (2009) Using molecular simulated to characterise metal-organic frameworks for adsorption applications. Chem Soc Rev 38:1237–1247
11. Diep P, Johnson JK (2000) An accurate H2–H2 interaction potential from first principles. J Chem Phys 112:4465–4473
12. Gagliardi L, Pyykko P (2004) How many hydrogen atoms can be bound to a metal? Predicted MH12 species. J Am Chem Soc 126:15014–15015
13. Chandrakumar KRS, Ghosh SK (2007) Electrostatics driven interaction of dihydrogen with s-block metal cations: theoretical prediction of stable MH16 complex. Chem Phys Lett 447:208–214
14. Kiran B, Kandalam AK, Jena P (2006) Hydrogen storage and the 18-electron rule. J Chem Phys 124:224703 (-1, -6)
15. Eley DD (1949) Mechanisms of hydrogen catalysis. Q Rev 3:209–225 (continued as Chem Soc Rev)
16. Kubas GJ (2007) Fundamentals of H_2 binding and reactivity on transition metals underlying hydrogenase function and H_2 production and storage. Chem Rev 107:4152–4205
17. Lochan RC, Head-Gordon M (2006) Computational studies of molecular hydrogen binding affinities: the role of dispersion forces, electrostatics, and orbital interactions. Phys Chem Chem Phys 8:1357–1370
18. Rowsell JLC, Millward AR, Park KS, Yaghi OM (2004) Hydrogen sorption in functionalized metal-organic frameworks. J Am Chem Soc 126:5666–5667
19. Ma SQ, Zhou H-C (2006) A metal-organic framework with entatic metal centers exhibiting high gas adsorption affinity. J Am Chem Soc 128:11734–11735

20. Eddaoudi M, Moler DB, Li H, Chen B, Reineke TM, O'Keeffe M, Yaghi OM (2001) Modular chemistry: secondary building units as a basis for the design of highly porous and robust metal-organic carboxylate frameworks. Acc Chem Res 34:319–330
21. O'Keeffe M, Peskov MA, Ramsden SJ, Yaghi OM (2008) The reticular chemistry structure resource (RCSR) database of, and symbols for, crystal nets. Acc Chem Res 41:1782–1789
22. Tranchemontagne DJ, Mendoza-Cortés JL, O'Keeffe M, Yaghi OM (2009) Secondary building units, nets and bonding in the chemistry of metal-organic-frameworks. Chem Soc Rev 38:1257–1283
23. Chae HK, Siberio-Pérez DY, Kim J, Go Y, Eddaoudi M, Matzger AJ, O'Keeffe M, Yaghi OM (2004) A route to high surface area, porosity and inclusion of large molecules in crystals. Nature 427:523–527
24. Sastre G, Corma A (2009) The confinement effect in zeolites. J Mol Catal A 305:3–7
25. Garberoglio G, Skoulidas AI, Johnson JK (2005) Adsorption of gases in metal organic materials: comparison of simulations and experiments. J Phys Chem B 109:13094–13103
26. Darkrim F, Levesque D (1998) Monte Carlo simulations of hydrogen adsorption in single-walled carbon nanotubes. J Chem Phys 109:4981–4984
27. Frost H, Düren T, Snurr RQ (2006) Effects of surface area, free volume, and heat of adsorption on hydrogen uptake in metal-organic frameworks. J Phys Chem B 110:9565–9570
28. Frost H, Snurr RQ (2007) Design requirements for metal-organic frameworks as hydrogen storage materials. J Phys Chem C 111:18794–18803
29. Yildirim T, Hartman (2005) Direct observation of hydrogen adsorption sites and nanocage formation in metal-organic frameworks. Phys Rev Lett 95:215504 (-1,-4)
30. Rowsell JLC, Yaghi OM (2006) Effects of functionalization, catenation, and variation of the metal oxide and organic linking units on the low-pressure hydrogen adsorption properties of metal-organic frameworks. J Am Chem Soc 128:1304–1315
31. Sagara T, Klassen J, Ortony J, Ganz E (2005) Binding energies of hydrogen molecules to isoreticular metal-organic framework materials. J Chem Phys 123:014701 (-1,-4)
32. Sagara T, Klassen J, Ganz E (2004) Computational study of hydrogen binding by metal-organic framework-5. J Chem Phys 121:12543–12547
33. Samanta A, Furuta T, Li J (2006) Theoretical assessment of the elastic constants and hydrogen storage capacity of some metal-organic framework materials. J Chem Phys 125:084714 (-1,-8)
34. Mulder FM, Dingemans TJ, Wagemaker M, Kearley GJ (2005) Modelling of hydrogen adsorption in the metal organic framework MOF5. Chem Phys 317:113–118
35. Bordiga S, Vitillo JG, Ricchiardi G, Regli L, Cocina D, Zecchina A, Arstad B, Bjørgen M, Hafizovic J, Lillerud KP (2005) Interaction of hydrogen with MOF-5. J Phys Chem B 109:18237–18242
36. Barbosa LAMM, Zhidomirov GM, van Santen RA (2001) Theoretical study of the molecular hydrogen adsorption and dissociation on different Zn(II) active sites of zeolites. Catal Lett 77:55–62
37. Negri F, Saendig N (2007) Tuning the physisorption of molecular hydrogen: binding to aromatic, hetero-aromatic and metal-organic framework materials. Theor Chem Acc 118:149–163
38. Klontzas E, Mavrandonakis A, Froudakis GE, Carissan Y, Klopper W (2007) Molecular hydrogen interaction with IRMOF-1: a multiscale theoretical study. J Phys Chem C 111:13635–13640
39. Rowsell JLC, Eckert J, Yaghi OM (2005) Characterization of H_2 binding sites in prototypical metal-organic frameworks by inelastic neutron scattering. J Am Chem Soc 127:14904–14910
40. Kuc A, Heine T, Seifert G, Duarte HA (2008) On the nature of the interaction between H_2 and metal-organic frameworks. Theor Chem Acc 120:543–550
41. Gomez D, Combariza AF, Sastre G (2009) Quantum-chemistry calculations of hydrogen adsorption in MOF-5. Phys Chem Chem Phys 11:9250–9258
42. Hirscher M, Panella B (2007) Hydrogen storage in metal-organic frameworks. Scripta Mater 56:809–812
43. Dailly A, Vajo JJ, Ahn CC (2006) Saturation of hydrogen sorption in Zn benzenedicarboxylate and Zn naphtalenedicarboxylate. J Phys Chem B 110:1099–1101
44. Sillar K, Hofmann A, Sauer J (2009) Ab initio study of hydrogen adsorption in MOF-5. J Am Chem Soc 131:4143–4150
45. Fu J, Sun H (2009) An ab initio force field for predicting hydrogen storage in IRMOF materials. J Phys Chem C 113:21815–21824
46. Han SS, Goddard WA (2007) Lithium-doped metal-organic frameworks for reversible H2 storage at ambient temperature. J Am Chem Soc 129:8422–8423
47. Wong M, Van Kuiken BE, Buda C, Dunietz BD (2009) Multiadsorption and coadsorption of hydrogen on model conjugated systems. J Phys Chem C 113:12571–12579
48. Buda C, Dunietz BD (2006) Hydrogen physisorption on the organic linker in metal organic frameworks: ab initio computational study. J Phys Chem B 110:10479–10484
49. Dincă M, Dailly A, Liu Y, Brown CM, Neumann DA, Long JR (2006) Hydrogen storage in a microporous metal-organic framework with exposed Mn^{2+} coordination sites. J Am Chem Soc 128:16876–16883
50. Sun YY, Kim Y-H, Zhang SB (2007) Effect of spin state on the dihydrogen binding strength to transition metal centers in metal-organic frameworks. J Am Chem Soc 129:12606–12607
51. Zhou W, Yildirim T (2008) Nature and tunability of enhanced hydrogen binding in metal-organic frameworks with exposed transition metal sites. J Phys Chem C 112:8132–8135
52. Kosa M, Krack M, Cheetham AK, Parrinello M (2008) Modelling the hydrogen storage materials with exposed M^{2+} coordination sites. J Phys Chem C 112:16171–16173
53. Dietzel PDC, Panella B, Hirscher M, Blom R, Fjellvag H (2006) Hydrogen adsorption in a nickel based coordination polymer with open metal sites in the cylindrical cavities of the desolvated framework. Chem Commun 959–961
54. Zhou W, Wu H, Yildirim T (2008) Enhanced H2 adsorption in isostructural metal-organic frameworks with open metal sites: strong dependence of the binding strength on metal ions. J Am Chem Soc 130:15268–15269
55. Vitillo JG, Regli L, Chavan S, Ricchiardi G, Spoto G, Dietzel PDC, Bordiga S, Zecchina A (2008) Role of exposed metal sites in hydrogen storage in MOFs. J Am Chem Soc 130:8386–8396
56. Wong-Foy AG, Matzger AJ, Yaghi OM (2006) Exceptional H2 saturation uptake in microporous metal-organic frameworks. J Am Chem Soc 128:3494–3495
57. Liu Y, Kabbour H, Brown CM, Neumann DA, Ahn CC (2008) Increasing the density of adsorbed hydrogen with coordinatively unsaturated metal centers in metal-organic frameworks. Langmuir 24:4772–4777
58. Kong L, Roman-Perez G, Soler JM, Langreth DC (2009) Energetics and dynamics of H2 adsorbed in a nanoporous material at low temperature. Phys Rev Lett 103:096103 (-1,-4)
59. Brown CM, Lin Y, Yildirim T, Peterson VK, Kepert CJ (2009) Hydrogen adsorption in HKUST-1: a combined inelastic neutron scattering and first-principles study. Nanotechnology 20:204025 (-1,-11)
60. Jhi S-H (2007) A theoretical study of activated nanostructured materials for hydrogen storage. Catal Today 120:383–388
61. Grimme S (2004) Accurate description of van der Waals complexes by density functional theory including empirical corrections. J Comput Chem 25:1463–1473